Published in final edited form as:
J Immunol. 2013 September 1; 191(5): 2372–2383. doi:10.4049/jimmunol.1300107.

MULTI-STAGE T CELL-DENDRITIC CELL INTERACTIONS CONTROL OPTIMAL CD4 T CELL ACTIVATION THROUGH THE ADAP-SKAP55 SIGNALING MODULE[1]

Jason S. Mitchell[*], **Brandon J. Burbach**[*], **Rupa Srivastava**[*], **Brian T. Fife**[¶], and **Yoji Shimizu**[*]
[*]Department of Laboratory Medicine and Pathology, University of Minnesota Medical School, Minneapolis, MN 55455

[¶]Department of Medicine, Center for Immunology, Masonic Cancer Center, University of Minnesota Medical School, Minneapolis, MN 55455

Abstract

The antigen-specific interactions between T cells and dendritic cells progress through dynamic contact stages *in vivo* consisting of early long-term stable contacts and later confined, yet motile, short-lived contacts. The signaling pathways that control *in vivo* interaction dynamics between T cells and dendritic cells during priming remain undefined. ADAP is a multi-functional adapter that regulates “inside-out” signaling from the T cell receptor to integrins. Using two-photon microscopy, we demonstrate that in the absence of ADAP, CD4 T cells make fewer early-stage stable contacts with antigen-laden dendritic cells, and the interactions are characterized by brief repetitive contacts. Furthermore, ADAP-deficient T cells show reduced contacts at the late motile contact phase and display less confinement around dendritic cells. The altered T cell interaction dynamics in the absence of ADAP are associated with defective early proliferation and attenuated T cell receptor signaling *in vivo*. Regulation of multi-stage contact behaviors and optimal T cell signaling involves the interaction of ADAP with the adapter SKAP55. Thus, integrin activation by the ADAP-SKAP55 signaling module controls the stability and duration of T cell-dendritic cell contacts during the progressive phases necessary for optimal T cell activation.

INTRODUCTION

Initiation of the T cell immune response involves recognition by the antigen-specific T cell receptor (TCR) complex of a combination of an antigenic peptide and a self major histocompatibility complex (MHC) protein expressed on the surface of dendritic cells (DCs)[2]. T cell activation requires physical contact between the T cell and the DC that is facilitated by adhesion molecules such as the integrin LFA-1 (1). T cell interactions with antigen-presenting cells that lead to T cell activation and clonal expansion are highly dynamic *in vivo* (2, 3). In the absence of antigen encounter, naïve T cells move rapidly through the T cell zone of lymph nodes (LNs), exhibiting a random walk migration. When contacting an antigen-laden DC, antigen-specific T cells reduce their rate of motility and eventually form prolonged contacts with DCs(4, 5). This stable phase of contact persists for

[1]This work was supported by National Institutes of Health grant R01 AI038474 (to Y.S.). Y.S. is also supported by the Harry Kay Chair in Biomedical Research at the University of Minnesota.

Corresponding Author: Yoji Shimizu, University of Minnesota Medical School, Campus Code 2641, 2101 6th St. SE, Minneapolis, MN 55414. TEL:612-626-6849, FAX: 612-625-2199, shimi002@umn.edu.

[2]Abbreviations used in this article: ADAP, adhesion and degranulation promoting adapter protein; CTO, Cell Tracker Orange; CTV, Cell Trace Violet; DC, dendritic cells; LN, lymph node; PD-1, programmed death-1; SKAPP55, src kinase-associated phosphoprotein of 55 kDa; TPLSM, two photon laser scanning microsopy

hours and while the T cells maintain dynamic movement over the DC, they are highly confined to the DC site (6). After approximately 24 hours, a time point when the T cell begins to proliferate, velocity increases and the cells regain motility that is characterized by "swarming" behavior around the DCs, making brief and sometimes repeated contacts (5).

These temporal phases of T cell contact with DCs during initial T cell activation have been observed for both CD4 and CD8 T cells (5, 6). Several studies have suggested that disruption of the stable contact phase can lead to changes in the quality of the ensuing T cell response. Antibody-mediated disruption of TCR signaling on CD4 T cells with an anti-MHC class II antibody during the early stable contact phase (6 hours) results in transient successive T-DC contacts and a pronounced defect in early T cell proliferation and effector differentiation (7). In contrast, disruption of T cell signaling at the later "swarming" phase (24 hours) does not alter early T cell activation. Imaging studies suggest that one mechanism of action of inhibitory receptors, such as CTLA-4 and PD-1, is alteration of T cell contacts with DCs through disruption of the TCR stop signal (8, 9). An analysis of CD8 T cells revealed a loss of stable T-DC contacts when the DC lacks expression of ICAM-1, a ligand for the LFA-1 integrin (10). The loss of these stable contacts resulted in impaired priming and survival of CD8 T cells. Overall, these studies suggest an important role for the initial stable contact phase of T-DC interactions for T cell activation *in vivo*. However, little is known about the intracellular signals emanating from the TCR that control these dynamic intercellular interactions *in vivo*.

The hematopoietic-specific adapter molecule ADAP (adhesion and degranulation promoting adapter protein; also known as Fyb or SLAP-120/130) regulates the rapid and transient activation of LFA-1 that occurs upon TCR engagement (11, 12). As a result, ADAP-deficient CD4 T cells exhibit a reduced ability to interact with antigen-pulsed antigen-presenting cells *in vitro* (13). Regulation of TCR signaling to integrins by ADAP requires the constitutive association of ADAP with another adapter, SKAP55 (src kinase-associated phosphoprotein of 55kDa) (14–16). The ADAP-SKAP55 signaling complex regulates TCR-mediated adhesion by targeting ADAP-SKAP55 to β2 integrin sites by the SKAP55 pleckstrin homology domain (17, 18). A distinct biochemical pool of ADAP that is not associated with SKAP55 can bind in a TCR-inducible fashion with the CARMA1 scaffold and thus participates in the regulated assembly of the CARMA1-Bcl10-Malt1 complex that is critical for NF-κB activation (15, 17). Although ADAP-deficient T cells exhibit impaired adhesion to antigen-presenting cells *in vitro* and impaired T cell proliferation both *in vitro* and *in vivo* (13, 15, 19), little is known about the role that ADAP and in particular ADAP-dependent signals to integrins play in regulating T-DC contacts *in vivo*. In this study, we utilized two-photon laser scanning microscopy (TPLSM) to examine the function of ADAP in regulating the multi-phase interactions of CD4 T cells with antigen-laden DCs during the first 24 hours of T cell activation. These studies revealed that impaired CD4 T cell activation in the absence of ADAP is associated with changes in all three phases of T-DC contact *in vivo*, including increased early motility in the presence of antigen, conversion of the stable contact phase to a period of repetitive transient contacts, and a failure to maintain confined swarming behavior at later time points. The latter two behaviors are regulated by the interaction of ADAP with SKAP55, implicating TCR-mediated integrin activation signals in the control of T-DC contact duration that dictates optimal T cell activation *in vivo*.

MATERIALS AND METHODS

Mice

DO11.10 wild-type and ADAP−/− mice (11) crossed to transgenic hCAR mice (20) on the BALB/c background were generated as previously described (16). DO11.10 ADAP−/− Rag −/− Thy 1.1/1.2 mice were also generated by crossing with DO11.10 Rag −/− Thy 1.1 mice.

Recipient BALB/c mice were purchased from the National Cancer Institute. Mice were housed in specific pathogen-free facilities and were used between 8 and 12 weeks of age. All experimental protocols involving the use of mice were approved by the Institutional Animal Care and Use Committee at the University of Minnesota.

Cell labeling

DO11.10 T cells were labeled with different intravital cell dyes for cell visualization using the following modified protocols (21, 22). Cells labeled with CellTrace Violet (CTV) (Invitrogen) were resuspended in PBS with 10% FBS at 1×10^7 cells/ml. CTV diluted in PBS was added 1:1 to the cells (7.5 μM and 3.75 μM final concentration for TPLSM and flow cytometry, respectively) and incubated at 37°C for 20 min. For CFSE labeling (carboxyfluorescein succinimidyl ester) (Invitrogen), cells were resuspended in PBS with 5% FBS at 2×10^7 cells/ml. CFSE diluted in PBS was added 1:1 to the cells (2.5 μM final concentration) and incubated at 25°C for 5 min. Cells labeled with Cell Tracker Orange (CTO) (Invitrogen) were resuspended in DMEM with 1% FBS (D1F) at 4×10^7 cells/ml. CTO diluted in D1F was added 1:1 to the cells (2.5 μM final concentration) and incubated at 37°C for 30 min. After dye incubation, all labeled cells were quenched by washing 2x with complete T cell media (RPMI 1640, 10% FBS, 100 U/ml Penicillin-Streptomycin, 1 mM sodium pyruvate, 55 μM β-mercaptoethanol, 2 mM L-glutamine). Dye switching was used in all assays to confirm that there were no adverse effects of the different labeling conditions.

In vivo T cell activation

We utilized a previously described *in vivo* ear priming model in this study (5). Briefly, chicken ovalbumin protein (OVA) was emulsified in incomplete Freund's adjuvant (Sigma) (IFA) using 2 glass syringes and an emulsifying hub. When the emulsion was used for imaging endogenous DCs, CFSE was incorporated at a final concentration of 1 mM. Mice were anesthetized with an intraperitonal ketamine injection and 10 μl of emulsion containing 2 μg of OVA (unless otherwise stated) was injected subcutaneously into both ears. At 24 – 72 hours after injection, either unlabeled or CTV-labeled Thy1.1+ wild-type DO11.10 and Thy1.1/1.2+ ADAP−/− DO11.10 T cells were co-transferred by intravenous injection and the ear draining cervical LNs were harvested at the indicated timepoints for analysis. For ICAM-1 blocking experiments, transferred cells were allowed to home to LNs for one hour before 200 μg of anti-ICAM-1 antibody (clone YN1.7.4, Bio X Cell) was injected i.p. Cell suspensions were stained for the transferred T cells and PD-1 expression with the following anti-mouse antibodies: FITC DO11.10 TCR (KJ1–26), PE PD-1, APC Thy 1.1, Pacific Blue Thy 1.2, APC-eFluor 780 CD4, PerCP-Cy5.5 dump (negative gating strategy using B220, CD8, CD11b, F4/80) (eBioscience), and proliferation was assessed by CTV dilution. In ADAP reconstitution experiments, wild-type and ADAP−/− hCAR+ DO11.10 T cells were purified and transduced with adenovirus as previously described(15–17, 19, 23) and co-transferred into primed recipients. To distinguish the co-transferred populations, ADAP−/− reconstituted cells were labeled with CTV and wild-type cells were labeled with CFSE.

For analysis of T cell signaling responses, draining LNs were harvested and immediately dissociated into 10 ml of 1.6% paraformaldehyde in PBS, fixed for 15 min at 25°C, then 40 ml of −20°C methanol was added to the cells and incubated on ice for 20 min as previously described (24). The cells were then stained for the transferred T cells as described above and also for phosphorylated c-Jun (Santa Cruz, #SC-822) and phosphorylated ribosomal S6 protein (Cell Signaling, #4854).

All samples were acquired on a LSR II flow cytometer (BD Biosciences) and analyzed using Flowjo software (Treestar).

Short-term *in vivo* cohoming assays

In vivo homing assays were performed using previously described methods (25). Briefly, recipient mice were primed in one ear with 1 μg OVA and IFA, and with IFA only in the contralateral ear. One day later, an equal number of CTV-labeled Thy1.2+ wild-type DO11.10 T cells and CTV-labeled Thy1.1/1.2+ ADAP−/− DO11.10 T cells were transferred by i.v. injection. Draining cervical lymph nodes and spleens were harvested at 4, 8 and 24 hours after transfer and the single cell suspensions labeled with FITC DO11.10 TCR (KJ1–26), APC Thy 1.1, APC-eFluor 780 CD4, PerCP-Cy5.5 dump (B220, CD8, CD11b, F4/80) (eBioscience) prior to flow cytometry. The homing index was calculated as previously described (26).

TPLSM acquisition and analysis

A Leica TCS MP resonance scanning microscope with 4 non-descanned photomultiplier detectors and a Mai Tai DeepSee two-photon laser (15W; Spectra-Physics) was used for *in vivo* imaging. Explanted draining LNs were immobilized on coverslips with the hilium facing away from the objective and maintained at 37°C using a heated chamber with circulated RPMI media bubbled with 95% O_2 5% CO_2. Samples were excited with the two-photon laser at 840nm and emission wavelengths of 450–490 nm (for CTV), 500–560 nm (for CFSE), and 584–676 nm (for CTO) were collected in the detectors. The xy acquisition dimensions were 193.75 μm x 193.75 μm and were scanned at 8000 Hz with a pixel resolution of 0.28 μm. Z-stacks of 100–150 μm at a 1.98 μm step-size were acquired every 30 sec for 30 min, at a minimum of 40 μm below the capsule (identified by second harmonic generation) and proximal to the afferent lymphatics as determined by the drainage of the CFSE/IFA emulsion. Image analysis and the identification of cell tracks and average track velocity was performed using Imaris 5.7.2×64 software (Bitplane). Contact time was determined by manually examining each T-DC interaction; no contact was scored if black pixels were visualized between the cells. Cell displacement was calculated using a Microsoft Excel written macro program written in Microsoft Visual Basic for Applications as previously described (8). The post-initial DC-contact confinement ratio (CR) was determined by first creating cell tracks that began at the point of T-DC contact termination, where only tracks that were visible for at least 5 minutes were analyzed. The CR was then created by dividing the cell displacement from origin (contact termination) by the total track length (27).

RESULTS

Impaired antigen-specific proliferation of ADAP-deficient CD4 T cells *in vivo*

To examine the role of ADAP in regulating T-DC contacts during T cell activation *in vivo*, we utilized an activation system that was previously used to define the three distinct stages of CD4 T cell motility during the initial 24 hours of T cell activation (4, 5). In this system, adoptively transferred CD4 T cells expressing the OVA-specific transgenic TCR DO11.10 were stimulated in naïve Balb/c recipients by an antigen-emulsion depot in the ear with OVA protein and IFA. As previously described, this ear priming results in antigen acquisition by skin-resident DCs and the subsequent migration of antigen-bearing activated DCs to the draining LN (5). Under these conditions, we observed dramatically impaired proliferation of ADAP-deficient DO11.10 T cells when compared to wild-type DO11.10 T cells responding to antigen in the same mouse at all time points examined (Fig. 1A) and at multiple antigen doses (Fig. 1B). Clonal expansion was also impaired with ADAP-deficient DO11.10 T cells (Fig. 1C). The activation phenotype of ADAP-deficient DO11.10 T cells differed from wild-type DO11.10 T cells, as expression of the inhibitory receptor PD-1, which is rapidly upregulated upon TCR stimulation (28), was reduced in the ADAP-

deficient T cells (Fig. 1D). Thus, ADAP-deficient T cells exhibit an attenuated proliferative response to antigen *in vivo* in this system.

We next assessed the antigen-specific activation of ADAP-deficient T cells during the first 24 hours of stimulation *in vivo*. As early as 4 hours after antigen stimulation *in vivo*, wild-type DO11.10 T cells exhibited robust phosphorylation of c-jun that was sustained at 12 and 24 hours after challenge (Fig. 2). In contrast, antigen challenge of ADAP-deficient DO11.10 T cells resulted in much lower levels of c-jun phosphorylation at all of the time points examined. These results are consistent with our *in vitro* studies demonstrating that TCR-dependent phosphorylation of c-jun is regulated by ADAP (19). To determine if other pathways downstream of the TCR were also impaired following antigen challenge of ADAP-deficient T cells *in vivo*, we examined phosphorylation of the S6 ribosomal protein (Fig. 2), which is dependent on activation of PI 3-kinase, mTOR and MAP kinase (29). Even though these pathways are not directly dependent on ADAP (11, 15), we also observed reduced S6 phosphorylation following activation of ADAP-deficient DO11.10 T cells *in vivo*. Together, these results suggest that multiple signaling pathways downstream of the TCR are attenuated *in vivo* in the absence of ADAP.

T cell basal motility is not dependent on ADAP

Since we observed that ADAP controls T cell proliferation and downstream TCR signaling *in vivo*, we tested the hypothesis that these deficits in activation are due to the loss of stable ADAP-mediated T-DC contacts. We utilized TPLSM to examine the motility of wild-type and ADAP-deficient CD4 T cells in the absence and presence of antigen. To visualize antigen-laden DCs, we immunized mice with the dye CFSE incorporated into the IFA emulsion during ear priming in order to label endogenous DCs that have acquired antigen (5). Wild-type and ADAP-deficient DO11.10 T cells were labeled with either CTO or CTV prior to transfer into mice. With the use of these three dyes, the interactions of both wild-type and ADAP-deficient DO11.10 T cells with DCs in the same LN could be visualized. We initially examined the motility of wild-type and ADAP-deficient CD4 T cells in the absence of antigen challenge. At four hours after transfer, both wild-type and ADAP−/− DO11.10 T cells moved at similar average velocities of 10.81 and 10.29 μm/min, respectively (Fig. 3A and movie 1). Both T cell populations displaced randomly, consistent with previously reported studies (5), suggesting that ADAP is dispensable for normal scanning behavior (Fig. 3B). These results indicate that ADAP is not required for basal motility of T cells in LNs.

ADAP-deficient T cells do not form stable contacts with antigen-bearing DCs

We next examined the effect of antigen on the motility and interaction dynamics of wild-type and ADAP−/− CD4 T cells. At 4 hours after T cell transfer, the presence of antigen-bearing DC resulted in a significant reduction in the average velocities of wild-type (3.3 μm/min) and ADAP-deficient T cells (4.3 μm/min) (Fig. 3A, movies 2 and 3). Although both T cell populations reduced their average velocity, we consistently observed a slightly higher velocity rate for ADAP-deficient T cells. This was not due to fewer ADAP−/− T cells encountering and initiating contact with DCs, as the percentage of T cell contacts with DCs was similar between wild-type and ADAP−/− T cells (data not shown). Indeed, ADAP−/− T cells making contacts with DCs also exhibited a statistically higher velocity than wild-type T cells making DC contacts (Fig. 3A) that did not result in significantly greater displacement (Fig. 3B). At the four hour time point, we frequently observed wild-type DO11.10 T cells stably engaged with the body of the DC (movies 2 and 3). In contrast, ADAP−/− T cells engaged the periphery of the DC, and contacts were transient and sometimes repetitive. Figure 3C depicts the interactions of two wild-type T cells and two ADAP−/− T cells with a single DC using a kymograph format (movie 2). This analysis shows that the wild-type T

cells maintained a stable interaction with the DC during the entire 30 minutes of imaging, while the ADAP−/− T cells displayed unstable, transient interactions. Analysis of additional wild-type and ADAP−/− T cells revealed a similar difference in behavior with multiple DCs (Fig. 3D and movie 3). When we assessed the total contact time with a DC, wild-type T cells had a two-fold greater average total contact time compared with ADAP−/− T cells (25.0 minutes versus 12.3 minutes) (Fig. 3E). We also observed that the total contact time for an individual ADAP−/− T cell was typically either very low (<10 minutes) or very high (>20 minutes). In the absence of antigen, CFSE- labeled DCs could still be identified in the draining LN, but the transferred CD4 T cells did not form stable contacts with the DCs (Fig. 3E and movie 1). Since a role for ADAP in T cell signaling may vary with the strength of the TCR signal, we also examined T cell-DC contacts at 4 hours after challenge with a high dose of antigen (5 μg). We increased the imaging time from 30 to 60 minutes in order to detect potential differences between wild-type and ADAP−/− T cells at this higher antigen dose. We found that increasing the antigen dose resulted in increased total average contact time for both wild-type and ADAP−/− T cells (Fig. 3F). However, the average contact time remained higher for wild-type T cells (46.0 min. for wild-type T cells vs. 30.7 min. for ADAP−/− T cells). These results indicate that ADAP is critical for long-lasting stable contacts with antigen-laden DCs at early time points.

Altered trafficking of naïve ADAP−/− T cells into LNs (30) might alter the kinetics of the interaction of ADAP−/− T cells with antigen-laden DCs in vivo. To examine this issue, we performed short-term in vivo cohoming assays (31). In the presence of IFA but no antigen, we observed a modest (∼15–20%) reduction in the homing of ADAP−/− T cells to the draining cervical LN that reached statistical significance only at 8 and 24 hours after T cell transfer (Supplemental Fig. 1). Similar results were observed in the presence of antigen, although homing of wild-type and ADAP−/− T cells was now comparable at the 24 hour time point. There was no defect in the trafficking of ADAP−/− T cells to the spleen (Supplemental Fig. 1). Since we observed some reduction in the trafficking of ADAP−/− T cells to LNs in the presence of Ag at the early time points (4 and 8 hr), we examined T cell-DC contacts at a slightly later time point of 8 hours after T cell transfer. Consistent with what we observed at 4 hours (Fig. 3E), wild-type T cells again displayed a higher total average contact time compared to ADAP−/− T cells (23.0 minutes vs 11.7 minutes) (Fig. 3G). In addition, analysis of individual T cells demonstrated that while most ADAP−/− T cells had low total contact times, a small number of ADAP−/− T cells had high levels of contact time comparable to many of the wild-type T cells

ADAP regulates contact time with DCs at later time points

We next examined the interaction dynamics of wild-type and ADAP−/− T cells at a later time point, 24 hours after transfer. At this time point, activated DO11.10 T cells begin blasting, regain motility and make infrequent short contacts with DCs (5). We also observed that both wild-type DO11.10 T cells (8.0 μm/min) and ADAP−/− T cells (8.6 μm/min) had a higher average velocity at 24 hours that was similar to previous reports of late stage velocity (Fig. 4A). The slightly higher average velocity of the ADAP−/− T cells compared to wild-type T cells in the presence of antigen at the 24 hour time point was not statistically significant. However, we continued to see differences in contact time with DCs between wild-type and ADAP−/− T cells at this later time point (Fig. 4B and movie 4). While the average contact time for wild-type T cells decreased from the earlier stable phase to 9.1 min, the average contact time for ADAP−/− T cells was even lower at 3.3 min (Fig. 4B and movie 4). Thus, while both wild-type and ADAP−/− T cells have transitioned to the late-stage swarming type interactions exemplified by an increased velocity at 24 hours, ADAP−/− T cells continue to establish more transient contacts with DCs than wild-type T cells.

ADAP−/− T cells do not confine their movement around a DC

Additional analysis of the motility behavior of control wild-type DO11.10 T cells at the 24 hour time point revealed that initial contact with a DC was subsequently followed by a confinement of the movement of the T cell to a region where the contact was terminated. Tracking analysis showed that a wild-type T cell interacted with a DC, then broke contact and migrated away, only to return to a region close to the DC (Fig. 4C and movie 5). In contrast, ADAP −/− T cells generally migrated in a linear path away from the DC following initial contact (Fig. 4C and movie 6). Since we could not determine the contact history of the T cell prior to its first observed contact with a DC, we analyzed T cell behavior only after the contact with the DC was observed. In addition, we focused our analysis on the first five minutes following termination of contact, as this was the minimum amount of time required for a T cell to return to a contact site. Many of the ADAP−/− T cells often migrated out of the field of view during the observation period, suggesting random walking behavior. When we applied these analysis parameters, we calculated the confinement ratio (CR) of the initial DC contact, where the total distance from the origin (terminated contact point) is divided by the total track length. Thus, a T cell moving in a straight line away from the origin will have a CR of 1 (32). When the 5 min post initial DC contact tracks of wild-type T cells were analyzed, the mean CR was 0.488 +/− 0.037. In contrast ADAP−/− T cells had a significantly higher mean CR of 0.640 +/− 0.048 (Fig. 4D). However, many wild-type T cells exhibited a more circuitous confinement and thus would often take longer than 5 min to return to the contact site (Fig. 4C and movie 7). Thus, we also determined the CR at the endpoint of each track in the 30 min movie. The endpoint CR was also higher for ADAP−/− T cells (0.523 +/− 0.048) compared to wild-type T cells (0.316 +/− 0.025) (Fig. 4D). Thus, ADAP −/− T cells exhibited less confinement to the regions in the LN where they had initially made contact with a DC.

ADAP-dependent regulation of CD4 T cell activation in response to antigen *in vivo* involves the SKAP55 binding region of ADAP

We previously demonstrated that different regions of ADAP control the regulation of integrin function and CARMA1-dependent signaling pathways following TCR stimulation (15, 16, 19, 23). To test the hypothesis that the impaired T cell proliferative responses of ADAP−/− T cells *in vivo* are specifically due to ADAP-dependent regulation of T-DC contacts *in vivo*, we examined the functional effect of re-expressing wild-type ADAP and an ADAP mutant with a small deletion of the proline-rich region of ADAP (aa 338–358) in primary DO11.10 ADAP−/− T cells. The proline-rich region of ADAP mediates the association of ADAP with SKAP55, but does not affect the TCR-inducible association of ADAP with CARMA1 and TAK1 (15, 16). As a result, expression of this ADAP mutant (ADAPΔ338) in ADAP−/− T cells does not restore the integrin-mediated T cell-APC conjugate defect but does restore ADAP-dependent signaling downstream of CARMA1 (16). We infected wild-type or ADAP−/− DO11.10 T cells expressing the hCAR transgene with a control adenovirus construct expressing a Thy1.1 marker gene alone or adenovirus constructs expressing Thy1.1 and either wild-type ADAP or the ADAPΔ338 mutant (Supplemental Fig. 2). We have previously shown that expression of wild-type ADAP, but not the ADAPΔ338 mutant, in ADAP−/− T cells results in the rescue of endogenous SKAP55 expression (16, 17). These T cell populations were transferred together with wild-type DO11.10 T cells infected with the control adenovirus. This population served as an internal control in our experiments. Figure 5A shows that ADAP−/− T cells infected with the control adenovirus retained an impaired proliferative response to OVA/IFA challenge *in vivo* when compared to wild-type T cells expressing the control adenovirus. In contrast, expression of wild-type ADAP in ADAP−/− T cells resulted in antigen-dependent proliferation that was comparable to the wild-type control T cell population. This was not

observed when we expressed the ADAPΔ338 mutant in ADAP−/− T cells. Similar results were observed when we examined antigen-dependent expression of PD-1 (Fig. 5A).

We also examined antigen-mediated changes in S6 ribosomal protein and c-jun phosphorylation in ADAP−/− T cells expressing either wild-type ADAP or the ADAPΔ338 mutant. When compared to the wild-type control T cell population in each recipient mouse, antigen challenge *in vivo* of ADAP−/− T cells expressing the control adenovirus or the ADAPΔ338 mutant resulted in impaired c-jun phosphorylation and S6 phosphorylation (Fig. 5B). In contrast, expression of wild-type ADAP restored c-jun and S6 phosphorylation after antigen challenge to levels similar to those seen in the control wild-type T cells. We further quantitated this result by normalizing phosphorylation to the response observed with the co-transferred wild-type T cells expressing the control adenovirus (Fig. 5C). Together, these results suggest a critical role for the SKAP55 binding site in ADAP in optimal T cell activation following antigen challenge *in vivo*.

The SKAP55 binding site in ADAP regulates stable T-DC contacts and T-DC contact time

We next examined the interaction dynamics of ADAP−/− T cells expressing wild-type ADAP or the ADAPΔ338 mutant. ADAP−/− T cells expressing either the control adenovirus or wild-type ADAP had similar average velocity (~10 μm/min) in the absence of antigen (Fig. 6A). At the four hour time point, antigen challenge resulted in a dramatic decrease in average velocity for both of these T cell populations. However, as observed with wild-type and ADAP−/− T cells, the control ADAP−/− T cells had a statistically higher average velocity than ADAP−/− T cells expressing wild-type ADAP (5.6 μm/min. vs. 3.7 μm/min.). ADAP−/− T cells infected with the control adenovirus exhibited a contact behavior similar to uninfected ADAP−/− T cells (Fig.6B and movie 8). These T cells typically engaged in short repetitive contacts at the periphery of the DC (red spot-marked cells). Reconstitution of ADAP −/− T cells with wild-type ADAP restored stable long term contacts, as these T cells (marked with a blue dot) rarely detached from the DC during the 30 min imaging period. Furthermore, expression of wild-type ADAP in ADAP−/− T cells resulted in an increase in total mean T cell-DC contact time from 11.6 min for control infected ADAP−/− T cells to 24.5 min for ADAP−/− T cells expressing wild-type ADAP (Fig. 6A). These contact time values are almost identical to what was observed when we analyzed wild-type and ADAP−/− T cells (Fig. 3E). Thus, expression of wild-type ADAP in ADAP −/− T cells recapitulates the stable contact behavior of wild-type CD4 T cells.

Analysis of ADAP−/− T cells expressing the ADAPΔ338 mutant revealed that in the absence of antigen, both ADAP−/− T cells expressing wild-type ADAP or the ADAPΔ338 mutant displayed similar mean velocities (Fig. 6C). In addition, both T cell populations had similar low mean velocities at the four hour time point following antigen challenge. This suggests that the higher mean velocity of ADAP−/− T cells in the presence of antigen is not regulated by the SKAP55 binding region of ADAP. In contrast to the results observed with expression of wild-type ADAP, expression of the ADAPΔ338 mutant in ADAP−/− T cells did not rescue the interaction dynamics with DCs. Similar to ADAP−/− T cells, the mean contact time was dramatically reduced compared to control T cells (12.0 min versus 22.8 minutes). The ADAP−/− T cells expressing the ADAPΔ338 mutant clearly exhibited less stable contact behavior (red labeled cells in movie 9), while the ADAP−/− T cells expressing wild-type ADAP remained stably engaged during the imaging period (blue labeled cells). At the 24 hour time point, ADAP−/− T cells expressing wild-type ADAP or the ADAPΔ338 mutant increased their mean velocity with antigen from the early stable contact phase to a higher velocity of ~8 μm/min (Fig. 6C). However, the ADAP−/− T cells expressing ADAPΔ338 retained a lower total contact duration time than the control T cell population (6.4 min vs 10.5 min, respectively). When we assessed the endpoint confinement ratio by calculating the confinement ratio from the entire post-DC contact cell track, ADAP

−/− T cells expressing ADAPΔ338 had a significantly higher post-DC confinement ratio (0.435 +/− 0.025) compared to the control T cells (0.322 +/− 0.037) (Fig. 6D). Thus, the SKAP55 binding site in ADAP is critical for the maintenance of early and late stable CD4 T cell-DC contacts and for the retention of antigen-specific T cells to late motile DC contact sites.

Inhibition of ICAM-1 reduces T cell contact time with antigen-laden DCs

To provide further evidence that the reduced interactions of ADAP−/− T cells with DCs is mediated by ADAP-dependent regulation of LFA-1, we examined the interaction of wild-type and ADAP−/− DO11.10 T cells with antigen-laden DCs in the presence of an inhibitory anti-ICAM-1 antibody. Since short-term trafficking of naïve T cells into LNs would likely be impaired with ICAM-1 blockade, we waited for an hour after T cell transfer before injecting the anti-ICAM-1 antibody and assessed T cell-DC contacts at 4 hours after T cell transfer. Treatment with the anti-ICAM-1 antibody resulted in individual wild-type T cells detaching from a DC during the imaging period (Fig. 7A and movie 10). In contrast, stable interactions of wild-type T cells with DCs were observed in the presence of an isotype control antibody (Fig. 7B and movie 11). ADAP−/− DO11.10 T cells exhibited unstable, transient interactions with a DC in the presence of either the isotype control antibody or the anti-ICAM-1 antibody (Fig. 7A and 7B). ICAM-1 blockade resulted in a reduction in the average contact time of wild-type T cells with DCs from 21.6 min. to 13.1 min (Fig. 7C). The total contact time of wild-type T cells with DCs in the presence of anti-ICAM-1 was slightly higher than the contact time of ADAP−/− T cells with DCs in the presence of an isotype control antibody (10.2 min.), but was not statistically significant. The difference in contact time between wild-type T cells in the presence of anti-ICAM-1 and ADAP−/− T cells was due to a subset of wild-type T cells that maintained stable contacts with DCs for the entire 30 min. imaging period (Fig. 7C). Interestingly, we also observed that ICAM-1 blockade resulted in a statistically significant reduction in the total average contact time of ADAP−/− T cells with DCs from 10.2 min. to 6.8 min. These results are consistent with the hypothesis that T cell-DC contacts are dependent on ADAP-mediated regulation of LFA-1.

DISCUSSION

The ADAP-SKAP55 signaling module mediates “inside-out” signaling from the TCR to integrins, thereby providing a mechanism by which antigen recognition can lead to enhanced integrin-dependent contacts between T cells and DCs. In this study, we demonstrate that the ADAP-SKAP55 signaling axis is critical for the dynamic motility and early (4 hours) stable contacts between CD4 T cells and DCs, as well as the later (24 hours) “swarming” contact phase and T cell confinement to DC contact sites during swarming. The changes in T cell contact interactions with DCs in the absence of ADAP are associated with impaired early T cell activation responses. Thus, ADAP-SKAP55 represents a key signaling pathway that controls the stability and duration of contact between CD4 T cells and DCs during the initial phases of T cell activation.

Other studies have also demonstrated that cell contact duration affects the quality and magnitude of an immune response. The loss of germinal center responses in mice lacking the adapter protein SAP is due to impaired duration of interactions between activated SAP-deficient CD4 T cells and activated B cells (33). Although our work suggests that ADAP-SKAP55 controls cell contact dynamics during the early phases of activation of naïve CD4 T cells via regulation of integrin function, activated CD4 helper T cells appear to utilize a distinct integrin-independent mechanism of adhesion to interact with activated B cells (34). Imaging studies have also provided evidence that inhibitory receptors, such as CTLA-4 (9) and PD-1 (8), attenuate T cell responses by inhibiting the duration of contact between T cells and DCs. Regulatory T cells have also been proposed to inhibit CD4 and CD8 T cell

activation by disrupting the interaction of these T cells with DCs (22). Tolerogenic activation conditions have been reported to result in more transient T cell contacts with DCs when compared to T cells activated under immunogenic conditions (24, 35), although this difference in interaction dynamics between these distinct types of activation conditions has not been consistently observed (36).

Our studies are consistent with a model where optimal CD4 T cell activation involves an early phase of ADAP-SKAP55-dependent stable contact with a DC. We suggest that this stable contact phase is initiated by TCR signals received during early transient contacts that result in increased functional activity of LFA-1, resulting in the ability of LFA-1 to mediate more stable contacts with DCs after a few hours of stimulation. In the absence of the ADAP-SKAP55 complex, T cell contacts with DCs remain transient and the cumulative signals received by the TCR remain suboptimal during this critical early phase of T cell activation. Our analysis of the interaction of wild-type T cells with DCs in the presence of ICAM-1 blockade is consistent with this model, as the presence of the anti-ICAM-1 antibody reduced the contact time of wild-type T cells with DCs to a level similar to that seen with ADAP−/− T cells. It is interesting to note that ICAM-1 blockade also caused a further decrease in the total contact time of ADAP−/− T cells with DCs. This suggests the possibility that there may be an additional pathway that regulates T cell-DC contacts *in vivo* that is independent of ADAP but still dependent on ICAM-1. Our previous studies of T cell interactions with antigen-presenting cells *in vitro* have also suggested the existence of an ADAP-independent pathway of integrin-mediated T cell adhesion. Similar to what we have observed in these *in vivo* studies, ADAP−/− DO11.10 T cells exhibit impaired adhesion to antigen-presenting cells *in vitro*. However, antibody-mediated inhibition of LFA-1 further inhibits conjugate formation between ADAP−/− T cells and antigen-presenting cells (13).

There also appears to be additional heterogeneity in the interaction dynamics of T cells with DCs *in vivo* that has been revealed by our analysis of ADAP−/− T cells. In our analysis of T cell-DC contact time, we observed that the total average contact time of individual ADAP−/− T cells with DCs was either very low, or less frequently, very high. This bimodal distribution of contact times was much more pronounced for ADAP−/− T cells than for wild-type T cells, and was observed at 4 and 8 hours after transfer, and at low and high antigen doses. This result indicates that some T cells are able to maintain stable contacts with DCs in the absence of ADAP. Since our experimental system utilized a method of labeling endogenous DCs, it is possible that T cell interactions with different types of DCs may be differentially dependent on ADAP. Identification of molecular mediators that control T cell-DC contacts *in vivo* independently of ADAP will be an important area of future investigation.

Another hallmark of these early interaction dynamics is the significant reduction in T cell velocity that occurs in response to antigen. Similar to wild-type T cells, ADAP-deficient T cells also exhibit this antigen-dependent reduction in velocity. TCR-mediated increases in intracellular calcium have been associated with this reduction in T cell motility (37, 38). Previous work showing normal calcium flux in TCR-stimulated ADAP−/− T cells (11) is consistent with ADAP not being a major regulator of this antigen-dependent reduction in motility. Even though ADAP−/− T cells reduced their velocity in response to antigen, the overall reduction in average velocity was always less pronounced for the ADAP−/− T cells. ADAP appears to be critical for this difference in velocity, as ADAP−/− T cells expressing wild-type ADAP show a drop in velocity in response to antigen that is similar to control wild-type T cells. ADAP−/− T cells expressing the ADAPΔ338 mutant also have a velocity drop similar to wild-type T cells, suggesting that a region of ADAP distinct from the SKAP55 binding site controls this differential velocity reduction in response to antigen.

At the later 24 hour time point, T cells regain their motility and "swarm" around DCs with generally short-lived contacts. The role that this behavior has in promoting T cell activation remains unclear, although T cell signaling that occurs at this later time point has been proposed to be important for cell cycle entry, sustained CD25 expression, and DTH responses (39, 40). The ADAP-SKAP55 signaling module plays a role in regulating T cell contact behavior at this later time point as well. Although ADAP−/− T cells also resume their motility and engage DCs with transient contacts after 24 hours, ADAP−/− T cells still exhibited reduced total cumulative contact time at this stage when compared to wild-type T cells. Furthermore, ADAP −/− T cells exhibited reduced swarming. Since both T cell populations were moving at equal relatively fast velocities, we were able to compare how each of the cell types could "swarm" back to a DC after termination of the initial contact. This analysis revealed that ADAP −/− T cells showed significantly less confinement and more straight-line movement after initial DC encounter. The mechanism by which ADAP controls this "swarming" behavior is not clear. It is possible that this swarming requires T cells to receive a certain threshold of TCR signal that is not obtained by ADAP−/− T cells due to the reduced ability of T cells to contact DCs in the absence of ADAP. Chemokines might also play a role in T cell swarming around DCs at the 24 hour time point. Thus, it is possible that early signals received by a T cell that lead to expression of certain chemokine receptors may not occur in the absence of ADAP. Alternatively, ADAP might regulate the response of T cells to chemokine-mediated signals involved in T-DC interaction dynamics. CCR7-mediated regulation of LFA-1 has recently been reported to be regulated by the ADAP-SKAP55 signaling module (30). Although this study reported a lower homeostatic velocity of naïve T cells in LNs, we did not observe any difference in the basal velocity of naïve ADAP−/− CD4 T cells when compared to wild-type naïve CD4 T cells. The reason for this discrepancy is not clear, although we note that the absolute velocity rates reported for wild-type and ADAP−/− CD4 T cells by Kliche et al. (30) in popliteal LNs are higher than we observed in our analysis of inflamed cervical LNs.

ADAP is a multi-functional adapter that exists in distinct biochemical pools defined by the constitutive association of a subset of ADAP molecules in a T cell with SKAP55. The pool of ADAP that is not associated with SKAP55 facilitates the TCR-inducible assembly of the CARMA1-Bcl10-Malt1 signalosome (15–17). As the SKAP55 binding site in ADAP is not required for ADAP-dependent regulation of CARMA1-dependent signaling pathways, (16) expression of the ADAPΔ338 mutant of ADAP in ADAP−/− T cells restores CARMA1-dependent signaling responses, such as NF-κB activation, but does not result in restoration of optimal inside-out signaling from the TCR to integrins. We previously found that stimulation of purified ADAP−/− T cells with anti-CD3 and anti-CD28 antibodies, an activation protocol that does not require integrin-dependent interactions with antigen-presenting cells, results in impaired c-jun phosphorylation that is dependent on the pool of ADAP that interacts with CARMA1 and not the ADAP-SKAP55 signaling module (19). However, in the context of an *in vivo* antigen challenge that is dependent on efficient T cell-DC interactions regulated by ADAP, we have found that antigen-mediated phosphorylation of c-jun is in fact dependent on the ADAP-SKAP55 signaling module. This result suggests that global TCR signaling is likely impaired due to the disruption of stable contacts of ADAP−/− T cells with DCs *in vivo*.

In summary, we have shown that optimal antigen-specific activation of CD4 T cells *in vivo* is dependent on ADAP-SKAP55-regulated stable contact of activated CD4 T cells with DCs and swarming of CD4 T cells around DCs. Thus, ADAP-SKAP55 represents a key signaling pathway that controls the stability and duration of contact between CD4 T cells and DCs during the initial phases of T cell priming, which ultimately dictates optimal T cell activation.

Supplementary Material

Refer to Web version on PubMed Central for supplementary material.

Acknowledgments

We thank J. Fiege and N. Zumwalde for helpful discussion, and T. Lee, F. Shoyama, S. Brandt, and S. Jin for mouse genotyping and colony maintenance.

REFERENCES

1. Burbach BJ, Medeiros RB, Mueller KL, Shimizu Y. T cell receptor signaling to integrins. Immunol. Rev. 2007; 218:65–81. [PubMed: 17624944]
2. Germain RN, Robey EA, Cahalan MD. A decade of imaging cellular motility and interaction dynamics in the immune system. Science. 2012; 336:1676–1681. [PubMed: 22745423]
3. Cahalan MD, Parker I. Choreography of cell motility and interaction dynamics imaged by two-photon microscopy in lymphoid organs. Annu. Rev. Immunol. 2008; 26:585–626. [PubMed: 18173372]
4. Miller MJ, Wei SH, Parker I, Cahalan MD. Two-photon imaging of lymphocyte motility and antigen response in intact lymph node. Science. 2002; 296:1869–1873. [PubMed: 12016203]
5. Miller MJ, Safrina O, Parker I, Cahalan MD. Imaging the single cell dynamics of $CD4^+$ T cell activation by dendritic cells in lymph nodes. J. Exp. Med. 2004; 200:847–856. [PubMed: 15466619]
6. Mempel TR, Henrickson SE, Andrian UHVon. T-cell priming by dendritic cells in lymph nodes occurs in three distinct phases. Nature. 2004; 427:154–159. [PubMed: 14712275]
7. Celli S, Lemaitre F, Bousso P. Real-time manipulation of T cell-dendritic cell interactions in vivo reveals the importance of prolonged contacts for CD4+ T cell activation. Immunity. 2007; 27:625–634. [PubMed: 17950004]
8. Fife BT, Pauken KE, Eagar TN, Obu T, Wu J, Tang Q, Azuma M, Krummel MF, Bluestone JA. Interactions between PD-1 and PD-L1 promote tolerance by blocking the TCR-induced stop signal. Nat. Immunol. 2009; 10:1185–1192. [PubMed: 19783989]
9. Schneider H, Downey J, Smith A, Zinselmeyer BH, Rush C, Brewer JM, Wei B, Hogg N, Garside P, Rudd CE. Reversal of the TCR stop signal by CTLA-4. Science. 2006; 313:1972–1975. [PubMed: 16931720]
10. Scholer A, Hugues S, Boissonnas A, Fetler L, Amigorena S. Intercellular adhesion molecule-1-dependent stable interactions between T cells and dendritic cells determine CD8+ T cell memory. Immunity. 2008; 28:258–270. [PubMed: 18275834]
11. Peterson EJ, Woods ML, Dmowski SA, Derimanov G, Jordan MS, Wu JN, Myung PS, Liu Q-H, Pribila JT, Freedman BD, Shimizu Y, Koretzky GA. Coupling of the TCR to integrin activation by SLAP-130/Fyb. Science. 2001; 293:2263–2265. [PubMed: 11567141]
12. Griffiths EK, Krawczyk C, Kong YY, Raab M, Hyduk SJ, Bouchard D, Chan VS, Kozieradzki I, Oliveira-dos-Santos AJ, Wakeham A, Ohashi PS, Cybulsky MI, Rudd CE, Penninger JM. Positive regulation of T cell activation and integrin adhesion by the adapter Fyb/Slap. Science. 2001; 293:2260–2263. [PubMed: 11567140]
13. Mueller KL, Thomas MS, Burbach BJ, Peterson EJ, Shimizu Y. Adhesion and degranulation promoting adapter protein (ADAP) positively regulates T cell sensitivity to antigen and T cell survival. J. Immunol. 2007; 179:3559–3569. [PubMed: 17785790]
14. Wang H, Moon EY, Azouz A, Wu X, Smith A, Schneider H, Hogg N, Rudd CE. SKAP-55 regulates integrin adhesion and formation of T cell-APC conjugates. Nat. Immunol. 2003; 4:366–374. [PubMed: 12652296]
15. Medeiros RB, Burbach BJ, Mueller KL, Srivastava R, Moon JJ, Highfill S, Peterson EJ, Shimizu Y. Regulation of NF-κB activation in T cells via association of the adapter proteins ADAP and CARMA1. Science. 2007; 316:754–758. [PubMed: 17478723]

16. Burbach BJ, Srivastava R, Medeiros RB, O'Gorman WE, Peterson EJ, Shimizu Y. Distinct regulation of integrin-dependent T cell conjugate formation and NF-κB activation by the adapter protein ADAP. J. Immunol. 2008; 181:4840–4851. [PubMed: 18802088]

17. Burbach BJ, Srivastava R, Ingram MA, Mitchell JS, Shimizu Y. The pleckstrin homology domain in the SKAP55 adapter protein defines the ability of the adapter protein ADAP to regulate integrin function and NF-κB activation. J. Immunol. 2011; 186:6227–6237. [PubMed: 21525391]

18. Raab M, Wang H, Lu Y, Smith X, Wu Z, Strebhardt K, Ladbury JE, Rudd CE. T cell receptor "inside-out" pathway via signaling module SKAP1-RapL regulates T cell motility and interactions in lymph nodes. Immunity. 2010; 32:541–556. [PubMed: 20346707]

19. Srivastava R, Burbach BJ, Mitchell JS, Pagan AJ, Shimizu Y. ADAP regulates cell cycle progression of T cells via control of cyclin E and cdk2 expression through distinct CARMA1-dependent signaling pathways. Mol. Cell. Biol. 2012; 32:1908–1917. [PubMed: 22411628]

20. Hurez V, Dzialo-Hatton R, Oliver J, Matthews RJ, Weaver CT. Efficient adenovirus-mediated gene transfer into primary T cells and thymocytes in a new coxsackie/adenovirus receptor transgenic model. BMC. Immunol. 2002; 3:4. [PubMed: 12019030]

21. Quah BJ, Warren HS, Parish CR. Monitoring lymphocyte proliferation in vitro and in vivo with the intracellular fluorescent dye carboxyfluorescein diacetate succinimidyl ester. Nat. Protoc. 2007; 2:2049–2056. [PubMed: 17853860]

22. Tang Q, Adams JY, Tooley AJ, Bi M, Fife BT, Serra P, Santamaria P, Locksley RM, Krummel MF, Bluestone JA. Visualizing regulatory T cell control of autoimmune responses in nonobese diabetic mice. Nat. Immunol. 2006; 7:83–92. [PubMed: 16311599]

23. Srivastava R, Burbach BJ, Shimizu Y. NF-κB activation in T cells requires discrete control of IκB kinase α/β (IKKα/β) phosphorylation and IKKγ ubiquitination by the ADAP adapter protein. J. Biol. Chem. 2010; 285:11100–11105. [PubMed: 20164171]

24. Katzman SD, O'Gorman WE, Villarino AV, Gallo E, Friedman RS, Krummel MF, Nolan GP, Abbas AK. Duration of antigen receptor signaling determines T-cell tolerance or activation. Proc. Natl. Acad. Sci. U. S. A. 2010; 107:18085–18090. [PubMed: 20921406]

25. DeNucci C, Pagan AJ, Mitchell JS, Shimizu Y. Control of α4β7 integrin expression and CD4 T cell homing by the β1 integrin subunit. J. Immunol. 2010; 184:2458–2467. [PubMed: 20118278]

26. Weninger W, Crowley MA, Manjunath N, Andrian UHVon. Migratory properties of naive, effector, and memory $CD8^+$ T cells. J. Exp. Med. 2001; 194:953–966. [PubMed: 11581317]

27. Sumen C, Mempel TR, Mazo IB, Andrian UHVon. Intravital microscopy: visualizing immunity in context. Immunity. 2004; 21:315–329. [PubMed: 15357943]

28. Fife BT, Pauken KE. The role of the PD-1 pathway in autoimmunity and peripheral tolerance. Ann. N. Y. Acad. Sci. 2011; 1217:45–59. [PubMed: 21276005]

29. Salmond RJ, Emery J, Okkenhaug K, Zamoyska R. MAPK, phosphatidylinositol 3-kinase, and mammalian target of rapamycin pathways converge at the level of ribosomal protein S6 phosphorylation to control metabolic signaling in CD8 T cells. J. Immunol. 2009; 183:7388–7397. [PubMed: 19917692]

30. Kliche S, Worbs T, Wang X, Degen J, Patzak I, Meineke B, Togni M, Moser M, Reinhold A, Kiefer F, Freund C, Forster R, Schraven B. CCR7-mediated LFA-1 functions in T cells are regulated by 2 independent ADAP/SKAP55 modules. Blood. 2012; 119:777–785. [PubMed: 22117043]

31. DeNucci CC, Shimizu Y. β1 integrin is critical for the maintenance of antigen-specific CD4 T cells in the bone marrow but not long-term immunological memory. J. Immunol. 2011; 186:4019–4026. [PubMed: 21357540]

32. Matheu MP, Cahalan MD, Parker I. Immunoimaging: studying immune system dynamics using two-photon microscopy. Cold Spring Harb. Protoc. 2011 2011.

33. Qi H, Cannons JL, Klauschen F, Schwartzberg PL, Germain RN. SAP-controlled T-B cell interactions underlie germinal centre formation. Nature. 2008; 455:764–769. [PubMed: 18843362]

34. Cannons JL, Qi H, Lu KT, Dutta M, Gomez-Rodriguez J, Cheng J, Wakeland EK, Germain RN, Schwartzberg PL. Optimal germinal center responses require a multistage T cell:B cell adhesion process involving integrins, SLAM-associated protein, and CD84. Immunity. 2010; 32:253–265. [PubMed: 20153220]

35. Hugues S, Fetler L, Bonifaz L, Helft J, Amblard F, Amigorena S. Distinct T cell dynamics in lymph nodes during the induction of tolerance and immunity. Nat. Immunol. 2004; 5:1235–1242. [PubMed: 15516925]

36. Shakhar G, Lindquist RL, Skokos D, Dudziak D, Huang JH, Nussenzweig MC, Dustin ML. Stable T cell-dendritic cell interactions precede the development of both tolerance and immunity in vivo. Nat. Immunol. 2005; 6:707–714. [PubMed: 15924144]

37. Bhakta NR, Lewis RS. Real-time measurement of signaling and motility during T cell development in the thymus. Semin. Immunol. 2005; 17:411–420. [PubMed: 16256363]

38. Wei SH, Safrina O, Yu Y, Garrod KR, Cahalan MD, Parker I. Ca^{2+} signals in $CD4^{+}$ T cells during early contacts with antigen-bearing dendritic cells in lymph node. J. Immunol. 2007; 179:1586–1594. [PubMed: 17641025]

39. Allenspach EJ, Lemos MP, Porrett PM, Turka LA, Laufer TM. Migratory and lymphoid-resident dendritic cells cooperate to efficiently prime naive CD4 T cells. Immunity. 2008; 29:795–806. [PubMed: 18951047]

40. Itano AA, McSorley SJ, Reinhardt RL, Ehst BD, Ingulli E, Rudensky AY, Jenkins MK. Distinct dendritic cell populations sequentially present a subcutaneous antigen to CD4 T cells and stimulate different aspects of cell-mediated immunity. Immunity. 2003; 19:47–57. [PubMed: 12871638]

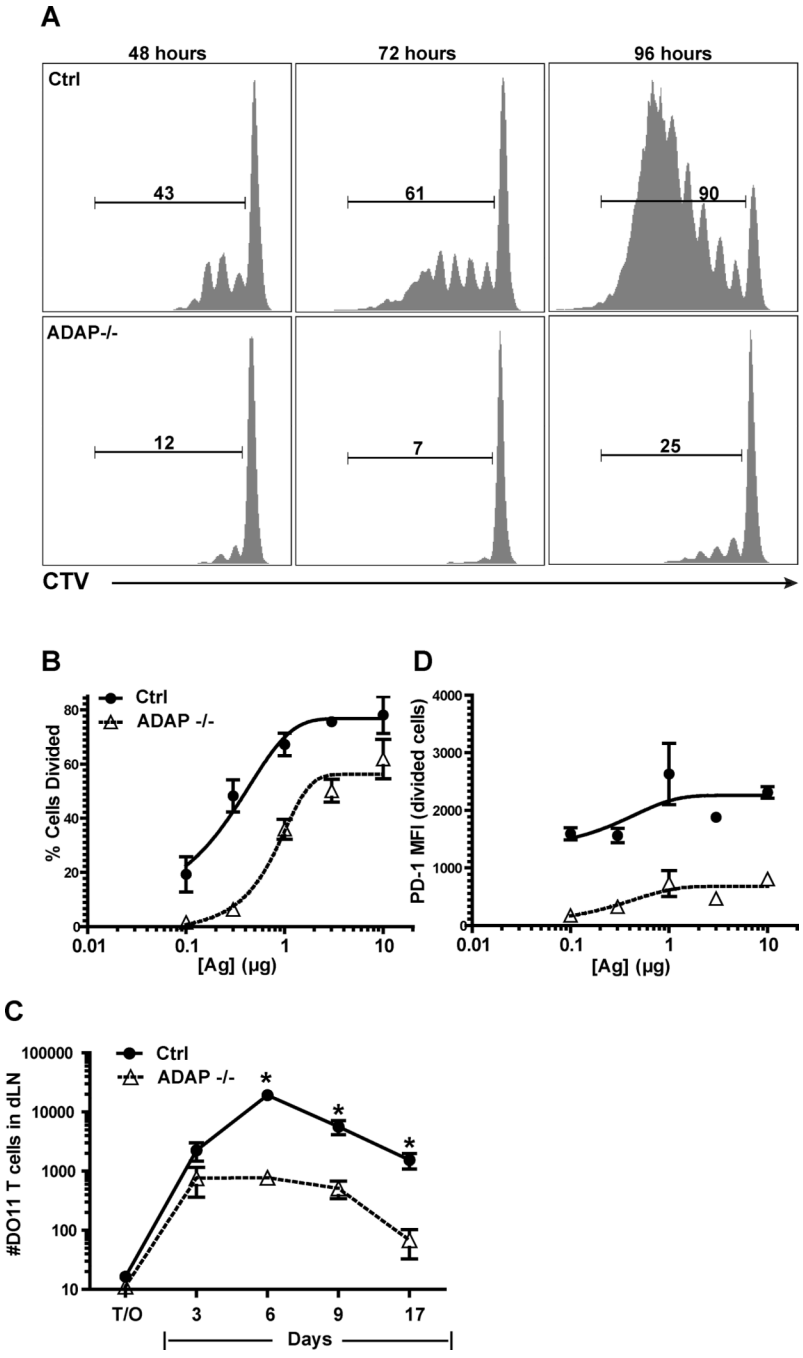

Figure 1. ADAP-deficient T cells show impaired antigen-dependent T cell activation *in vivo*

CTV-labeled wild-type and ADAP−/− DO11.10 T cells (200,000 T cells each) were co-transferred into IFA/OVA primed hosts. (A) Proliferation in the draining LNs was assessed at different times. Proliferation (B) and PD-1 expression (D) was assessed at 48 hours post-transfer at different antigen concentrations. (C) CTV-labeled wild-type and ADAP−/− DO11.10 T cells (10,000 cells each) were co-transferred into IFA/OVA ear primed hosts. Clonal expansion in the draining LNs was assessed at the indicated times. All plots are each representative of at least 3 independent experiments. *, P<0.05 unpaired t test.

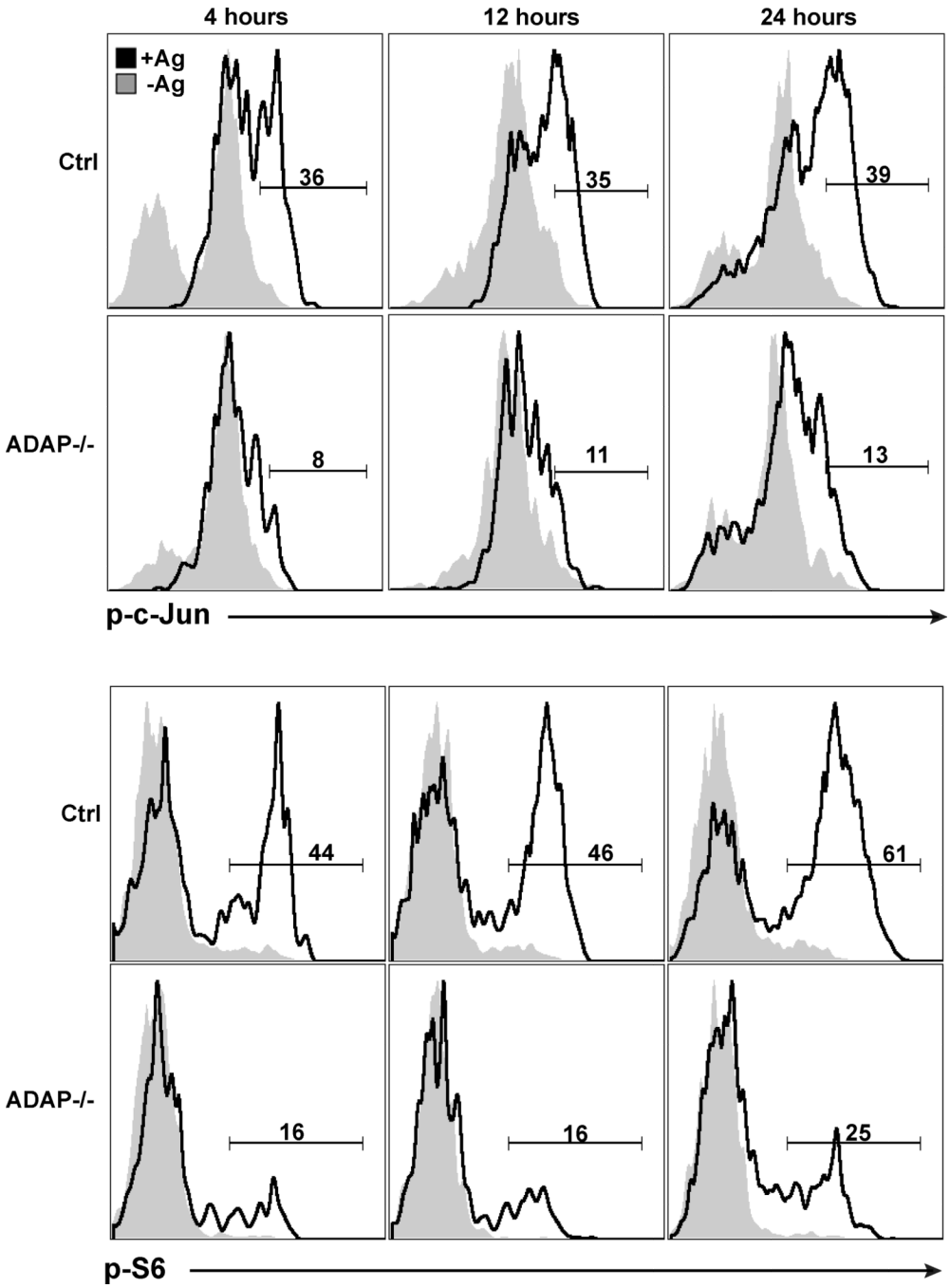

Figure 2. DAP-deficient T cells show impaired early TCR signaling following antigen challenge *in vivo*

Wild-type and ADAP−/− DO11 T cells (200,000 T cells) were co-transferred into recipient mice challenged with either IFA alone (shaded histograms, -Ag) or IFA/OVA (black histograms, +Ag) in the ear. Draining LNs were harvested at the indicated time points, fixed and stained for phosphorylated c-Jun and S6. Plots are representative of 4 independent experiments.

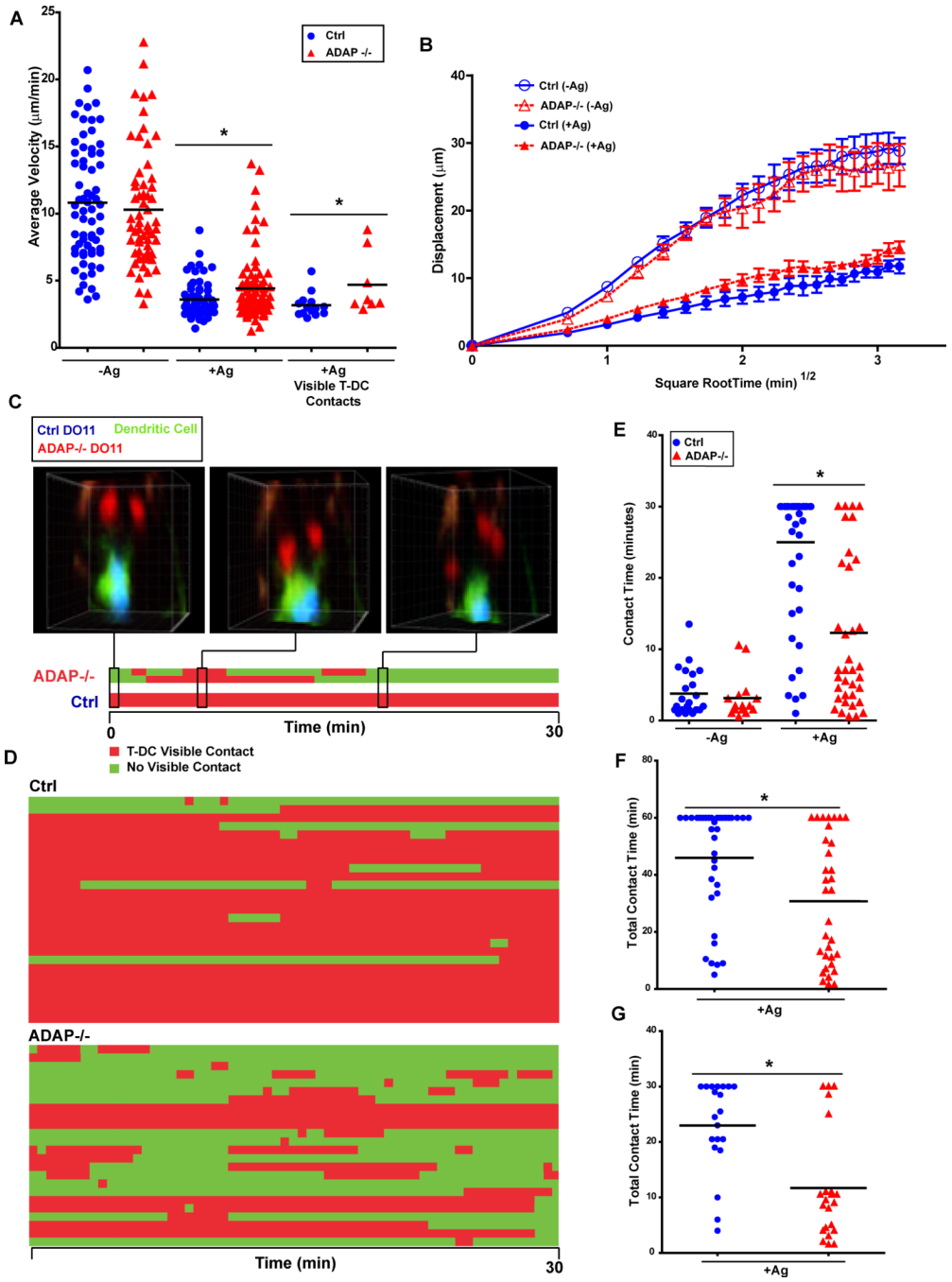

Figure 3. ADAP-deficient T cells do not form early stable contacts with cognate DCs *in vivo*

CTV-labeled wild-type (blue) and CTO-labeled ADAP−/− (red) DO11.10 T cells (3×10^6 cells each) were co-transferred into CFSE/IFA ear-primed recipients, with or without 1 μg OVA antigen (Ag), and draining LNs were harvested four hours after transfer and imaged by TPLSM. Average track velocity (A) and cell displacement (B) of individual movies representative of at least 5 independent experiments. (C) Three-dimensional images and corresponding kymograph of a single CFSE-labeled DC (green) interacting with 2 wild-type (blue) and 2 ADAP −/− (red) DO11 T cells. (D) Kymograph of T-DC interactions with multiple DCs from a single acquired movie. (E) Pooled cumulative T-DC contact time at 4 hours after antigen challenge from three separate movies. (F) Pooled cumulative T-DC

contact time at 4 hours after challenge with a high dose of antigen (5 μg) from three separate movies. (G) Pooled cumulative T-DC contact time at 8 hours after challenge with 1 μg OVA from three separate movies. *, $P<0.05$ unpaired t test.

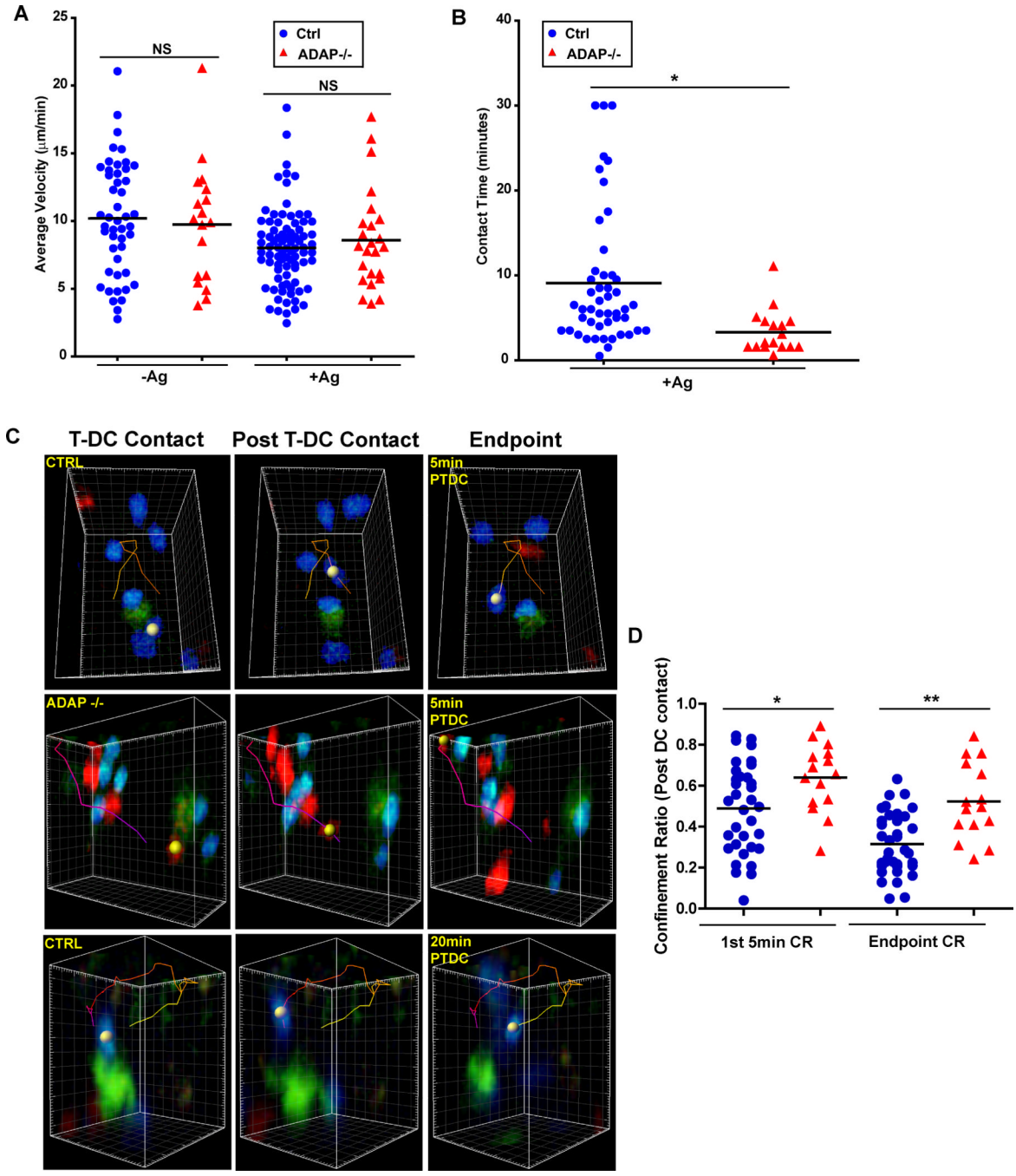

Figure 4. ADAP-deficient T cells are not confined near DC contact sites at the late swarming contact phase

CTV-labeled wild-type (blue) and CTO-labeled ADAP−/− (red) DO11.10 T cells (1×10^6 cells each) were co-transferred into CFSE/IFA ear-primed recipients, with or without OVA antigen (Ag), and draining LNs were harvested 24 hours after transfer and imaged by TPLSM. (A) Average track velocity of individual movies from 3 independent experiments. (B) Pooled cumulative T cell-DC contact time from three independent experiments. (C) Three-dimensional images of CFSE-labeled DCs (green) interacting with wild-type (blue) and ADAP−/− (red) DO11.10 T cells. The images show the initial T cell-DC contact, the contact termination or post T cell-DC contact, and the endpoint displacement of the cell after

5 min or 20 min. (D) The pooled confinement ratio of the tracks described in (C) from 3 independent experiments. *, P<0.05; **, P=0.001 unpaired t test.

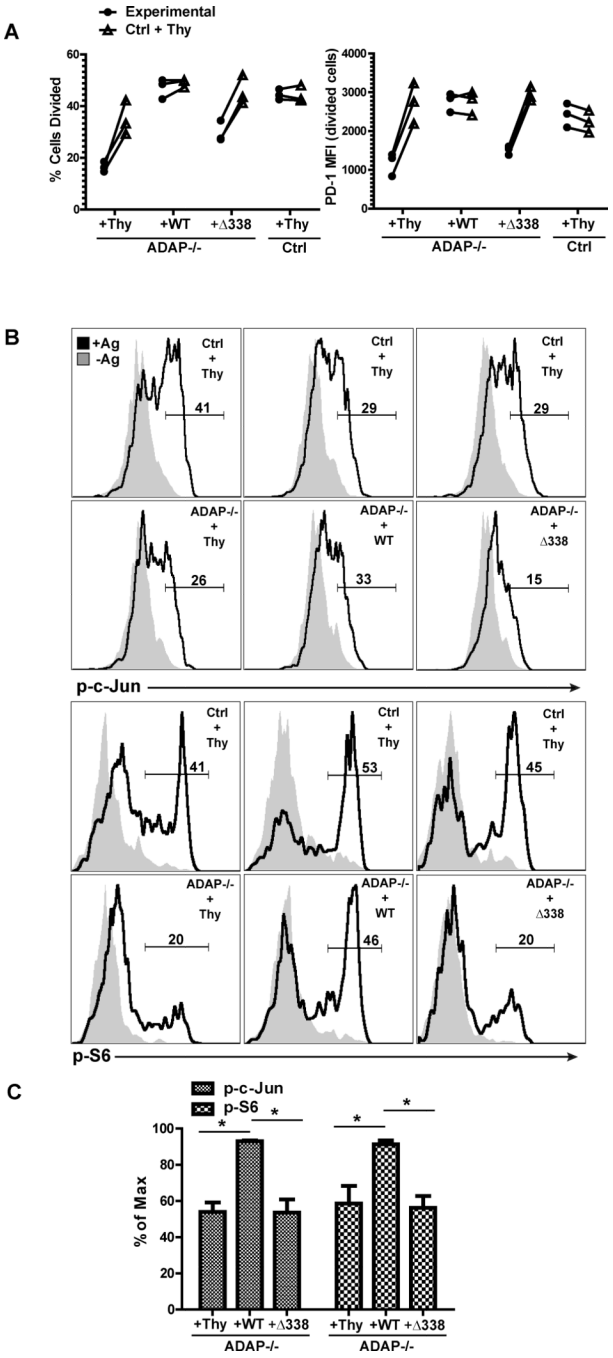

Figure 5. The SKAP55 binding region in ADAP regulates early T cell activation *in vivo*

Primary ADAP−/− DO11.10 hCAR T cells were transduced with control adenovirus expressing Thy1.1 or adenovirus expressing Thy1.1 and either wild-type ADAP or the ADAPΔ338 mutant as described in Methods. ADAP−/− reconstituted cells were co-transferred with wild-type DO11.10 hCAR T cells transduced with control adenovirus expressing Thy1.1 into OVA/IFA primed mice. (A) Proliferation in draining LNs was determined by CFSE (Ctrl + Thy; wild-type DO11.10 T cells transduced with control Thy1.1 adenovirus) and CTV (Experimental; ADAP−/− DO11.10 T cells transduced with the indicated adenovirus) dilution 48 hours after transfer. Cell samples were also stained for PD-1 expression. (B) Draining LNs were harvested at 4 hours after transfer, fixed and

stained for phosphorylated c-Jun and S6. (C) Intracellular staining for phosphorylated c-Jun and S6 from 3 independent experiments as in (B) normalized to the maximum response in each mouse (response of wild-type DO11.10 T cells transduced with control adenovirus). *, $P<0.05$ unpaired t test.

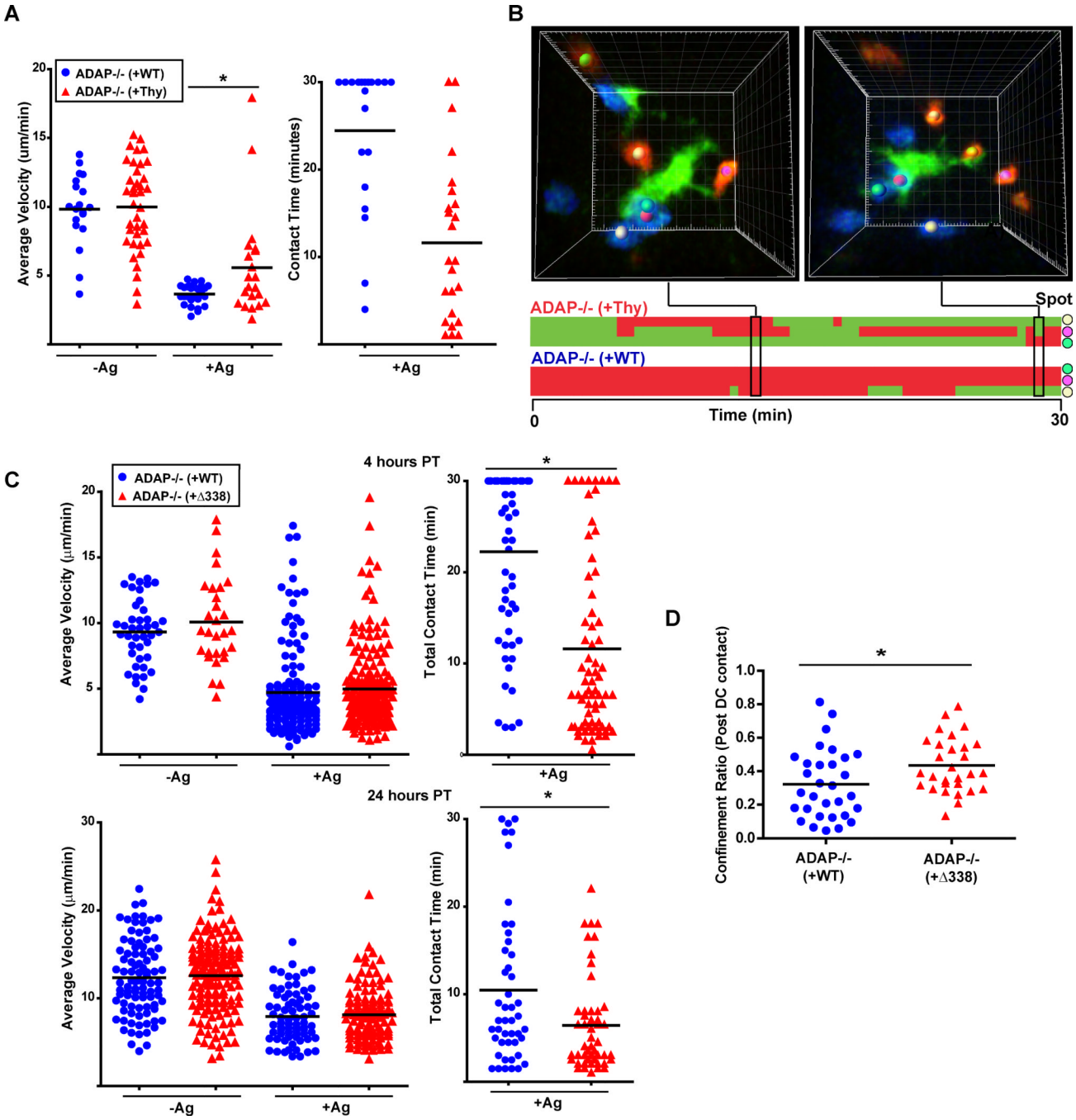

Figure 6. The SKAP55 binding region in ADAP regulates stable contacts and late stage DC confinement

Primary ADAP−/− DO11.10 hCAR T cells were transduced with control adenovirus expressing Thy1.1 or adenovirus expressing Thy1.1 and either wild-type ADAP or the ADAPΔ338 mutant as described in Methods. (A) ADAP−/− DO11.10 T cells transduced with control Thy1.1 adenovirus were labeled with CTO (red) and co-transferred with ADAP −/− DO11.10 T cells transduced with adenovirus expressing Thy1.1 and wild-type ADAP and labeled with CTV (blue) into mice primed with CFSE/IFA with or without OVA antigen (Ag). Graphs show average velocity and T-DC contact time from 3 independent movies at four hours post T cell transfer. (B) Three-dimensional images and corresponding kymograph

of a single DC interacting with transferred T cells at 4 hours after transfer. Colored spots match cell images to contacts on the kymograph. (C) CTO-labeled ADAP−/− DO11.10 T cells transduced with ADAPΔ338 adenovirus (red) were co-transferred as in (A) with CTV-labeled ADAP−/− DO11.10 T cells transduced with wild-type ADAP adenovirus (blue). Graphs show average velocity and T-DC contact time from 3 independent movies at 4 hours (top) and 24 hours (bottom) post T cell transfer. (D) Pooled post-T cell-DC contact endpoint confinement ratio from 3 independent movies at 24 hours post-transfer for ADAP−/− DO11.10 T cells transduced with wild-type ADAP (blue) and ADAP−/− DO11.10 T cells transduced with ADAPΔ338 adenovirus (red). *, $P<0.05$ unpaired t test.

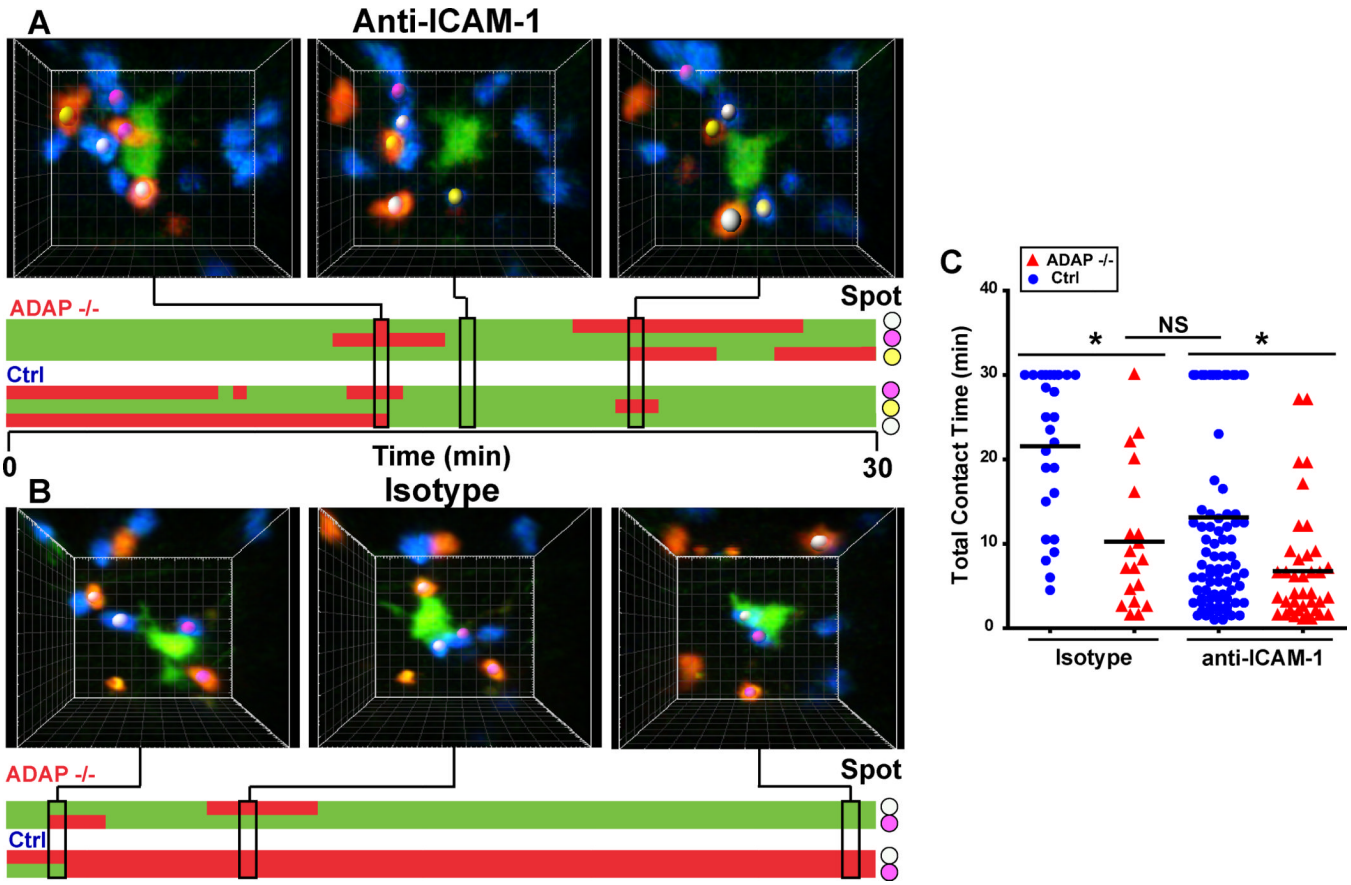

Figure 7. Inhibition of ICAM-1 reduces T cell contact time with antigen-laden DCs

CTV-labeled wild-type (blue) and CTO-labeled ADAP−/− (red) DO11.10 T cells were co-transferred into CFSE/IFA ear-primed recipients with OVA antigen (Ag). One hour after T cell transfer, 200 μg of anti-ICAM-1 antibody or isotype control antibody was administered by i.p. injection. Draining LNs were harvested 3 hours after antibody treatment and imaged by TPLSM. (A, B) Three-dimensional images and corresponding kymographs of a single DC interacting with transferred T cells in the presence of anti-ICAM-1 antibody (A) or isotype control antibody (B). Colored spots match cell images to contacts on the kymograph. (C) Pooled cumulative T-DC contact time from three separate movies. *, $P<0.05$ unpaired t test.